Advanced Imaging Assessment of Bone Quality

HARRY K. GENANT AND YEBIN JIANG

Osteoporosis and Arthritis Research Group, University of California, San Francisco, California 94143, USA

ABSTRACT: Noninvasive and/or nondestructive techniques can provide structural information about bone, beyond simple bone densitometry. While the latter provides important information about osteoporotic fracture risk, many studies indicate that bone mineral density (BMD) only partly explains bone strength. Quantitative assessment of macrostructural characteristics, such as geometry, and microstructural features, such as relative trabecular volume, trabecular spacing, and connectivity, may improve our ability to estimate bone strength. Methods for quantitatively assessing macrostructure include (besides conventional radiographs) dual X ray absorptiometry (DXA) and computed tomography (CT), particularly volumetric quantitative computed tomography (vQCT). Methods for assessing microstructure of trabecular bone noninvasively and/or nondestructively include high-resolution computed tomography (hrCT), microcomputed tomography (micro-CT), high-resolution magnetic resonance (hrMR), and micromagnetic resonance (micro-MR). vQCT, hrCT, and hrMR are generally applicable *in vivo*; micro-CT and micro-MR are principally applicable *in vitro*. Despite progress, problems remain. The important balances between spatial resolution and sampling size, or between signal-to-noise and radiation dose or acquisition time, need further consideration, as do the complexity and expense of the methods versus their availability and accessibility. Clinically, the challenges for bone imaging include balancing the advantages of simple bone densitometry versus the more complex architectural features of bone, or the deeper research requirements versus the broader clinical needs. The biological differences between the peripheral appendicular skeleton and the central axial skeleton must be further addressed. Finally, the relative merits of these sophisticated imaging techniques must be weighed with respect to their applications as diagnostic procedures, requiring high accuracy or reliability, versus their monitoring applications, requiring high precision or reproducibility.

KEYWORDS: osteoporosis; micro-imaging; micro-CT; micro-MRI; bone microarchitecture; bone quality

Address for correspondence: Harry K. Genant, University of California, San Francisco, San Francisco, CA 94143.
e-mail: harry.genant@ucsf.edu

Ann. N.Y. Acad. Sci. 1068: 410–428 (2006).
doi: 10.1196/annals.1346.038

INTRODUCTION

More than standard bone densitometry,[1] noninvasive and/or nondestructive techniques are capable of providing macro- or microstructural information about bone.[2] While the bone densitometry provides important information about osteoporotic fracture risk, numerous studies indicate that bone strength is only partially explained by bone mineral density (BMD). Quantitative assessment of macrostructural characteristics, such as geometry, and microstructural features, such as relative trabecular volume, trabecular spacing, and connectivity, may improve our ability to estimate bone strength.

The methods available for quantitatively assessing macrostructure include computed tomography (CT) and particularly volumetric quantitative computed tomography (vQCT). Noninvasive and/or nondestructive methods for assessing microstructure of trabecular bone include high-resolution computed tomography (hrCT), microcomputed tomography (micro-CT), high-resolution magnetic resonance (hrMR), and micromagnetic resonance (micro-MR). vQCT, hrCT, and hrMR are generally applicable *in vivo*, micro-CT and micro-MR are principally applicable *in vitro*.

VOLUMETRIC CT

The use of standard QCT has centered on a two-dimensional characterization of vertebral trabecular bone, but there is also interest in developing three-dimensional, or vQCT techniques to improve spinal measurements and to extend QCT assessments to the proximal femur (FIG. 1, 2). These three-dimensional techniques encompass the entire object of interest with stacked slices or spiral CT scans, and can use anatomic landmarks to automatically define coordinate systems for reformatting CT data into anatomically relevant projections.

Volumetric CT can determine bone mineral content (BMC) or BMD of the entire bone or subregion, such as a vertebral body or femoral neck, as well as provide separate analysis of the trabecular or cortical components. Since a true and highly accurate volumetric rendering is provided, important geometrical and biomechanically relevant assessments, such as cross-sectional moment of inertia and finite-element analyses can be derived.[2–8] Highly accurate assessment of bone size and density, independent of the artifacts of projectional radiographic and densitometric techniques (such as absorptiometry), can also be derived for epidemiologic studies and for studies of nutritional, racial, and genetic influences on bone size and density.[9]

Because of the complex anatomy of the proximal femur and its dramatic three-dimensional variations in bone density, vQCT has particularly important ramifications for both research and clinical applications at this biologically relevant site. vQCT and finite-element analysis modeling have been used by Lotz

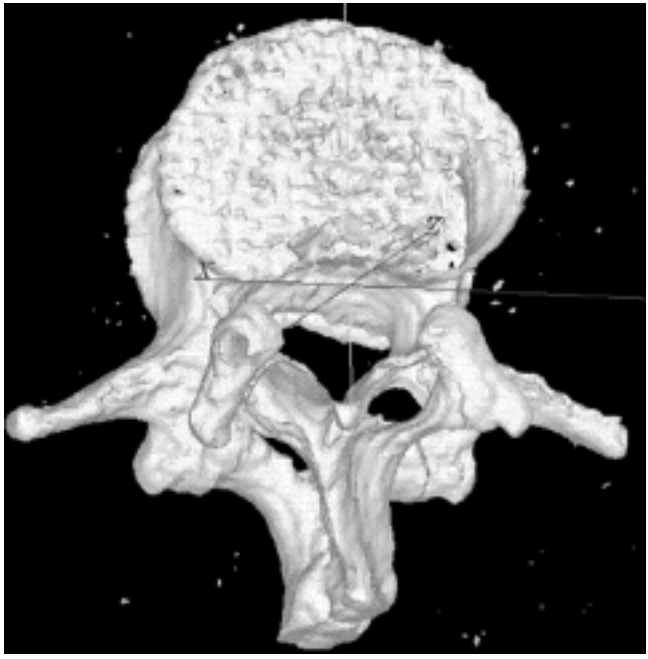

FIGURE 1. Volumetric QCT of the spine may be used to analyze bone mineral density in bone compartments and to accurately measure vertebral geometry. (Courtesy of Thomas Lang.)

et al.[7] and by Keyak *et al.*[4] to improve estimations of proximal femoral strength over global projectional densitometry. *In vitro* studies by Lang *et al.*[5,6] have shown enhanced prediction of *in vitro* fracture load using subregional vQCT of the hip. QCT three-dimensional finite-element model of the proximal femur shows moderate reproducibility in postmenopausal women.[10] QCT-based finite-element models of the hip in 51 women aged 74 ($\pm$5) years showed different risk factors for hip fracture during single-limb stance and falls, which agree with epidemiologic findings of different risk factors for cervical and trochanteric fractures.[11]

Finite-element models derived from QCT scans may improve the prediction of vertebral strength because they mechanically integrate all the geometrical and material property data within the scans. QCT BMD values of each bone voxel can be converted into elastic modulus values using predetermined correlation between the elastic modulus and QCT-derived BMD. Finite-element models integrate mechanically all of the anisotropic, inhomogeneous, and complex geometry of the bone structure examined. It has been demonstrated that voxel-based finite-element model-derived estimates of strength are better predictors of *in vitro* vertebral compressive strength than clinical measures of bone density derived from QCT with or without geometry.[12] Though imaging

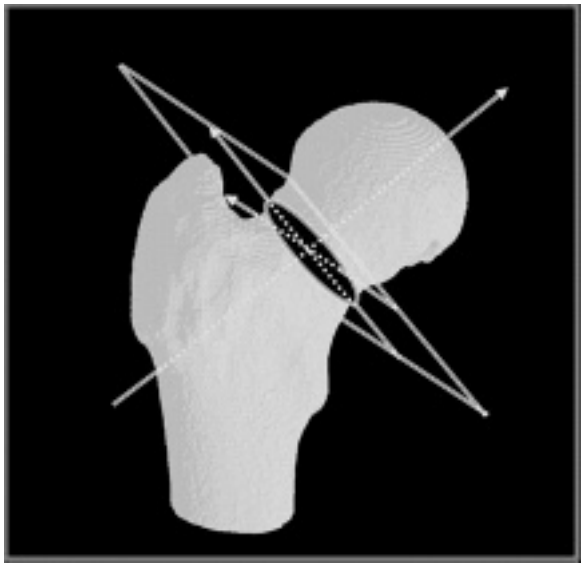

FIGURE 2. vQCT of the hip may be used to analyze BMD in bone compartments and to accurately measure proximal femoral geometry, as well as, to provide a basis for finite-element analyses. (Courtesy of Klaus Engelke.)

resolution is not critical in cross-sectional studies using clinical CT scanners, longitudinal studies that seek to track more subtle changes in stiffness over time should account for the small but highly significant effects of voxel size.[13] However, these data were generated in the laboratory with excised bone specimen without soft tissue: this remains to be confirmed from clinical studies and from epidemiology studies. In addition, the compressive loading experiments used in the laboratory differ from *in vivo* conditions.

HIGH-RESOLUTION COMPUTED TOMOGRAPHY

There is much research under way in the areas of hrCT (micro-CT). The spatial resolution of clinical CT scanners (typically >0.4 mm) is inadequate for highly accurate cortical measurements and for the analysis of discrete trabecular morphological parameters, and new CT developments address this issue. There are two main approaches: the development of new image acquisition and analysis protocols using state-of-the-art clinical CT scanners; and the development of new hrCT scanners for *in vivo* investigations of the peripheral skeleton, or of new micro-CT scanners for *in vitro* two- or three-dimensional structural analysis of very small bone samples (typically <2 cm^3).

State-of-the-art spiral CT scanners use a relatively high resolution (≈ 0.4 mm $\times$ 0.4 mm), thin slice (1–1.5 mm) to provide images of the spine and hip that clearly display structural information. However, it requires a higher

radiation exposure than is employed for standard QCT. Also, the extraction of the quantitative structural information is difficult and the results vary substantially according to the threshold and image processing techniques used. This is due to substantial partial volume effects at this resolution relative to the typical dimensions of trabeculae (100–400 μm) and trabecular spaces (200–2000 μm). hrCT has been employed to measure a feature called the trabecular fragmentation index (length of the trabecular network divided by the number of discontinuities) in an effort to separate osteoporotic subjects from normal subjects,[14] and a similar trabecular textural analysis approach has been reported by Ito *et al.*[15] Gordon *et al.*[16] reported on a hrCT technique that extracted a texture parameter reflecting trabecular hole area, analogous to star volume that appears to enhance vertebral fracture discrimination relative to BMD (FIG. 3). One *in vitro* study showed that a combination of BMD and trabecular structural parameters of bone cubes examined by pQCT improved prediction of bone biomechanical properties.[17] Recently, Link' group has provided a comprehensive analysis of multislice hrCT with hrMR applied to the peripheral skeleton.[18]

High-resolution spinal CT with postprocessing steps used to assess trabecular structure from CT image (A). The structure is segmented by defining the boundary between cortical and trabecular bone (B). The trabecular network is reduced to a binary image (C), which is then thinned to produce a representation of the trabecular form (D).

Higher-resolution CT scanners for peripheral skeletal measurements *in vivo* have been developed and evaluated by Rüegsegger, Durand, and Müller.[19–21] The images show trabecular structure in the radius, with a spatial resolution of 170 μm isotropic. The images can be used for quantitative trabecular structure analysis and also for a separate assessment of cortical and trabecular BMD. Note, however, that these state-of-the-art scanners approach the limits of spatial resolution achievable *in vivo* with acceptable radiation exposure.[22]

More recent studies of high-resolution and volumetric CT have further documented the unique capabilities of these techniques. They have shown that trabecular structural analysis from multi-detector row CT images can better discriminate postmenopausal women with vertebral fracture than dual X ray absorptiometry (DXA).[23] High-resolution spiral CT assessment of the trabecular structure of the vertebral body in combination with BMD improves prediction of biomechanical properties.[24] In elderly men, there is an independent association of sex steroid levels with cortical and trabecular area and their QCT volumetric BMD, but lack such association in young men.[25]

MICROCOMPUTED TOMOGRAPHY

To achieve very high-spatial resolution images, Feldkamp *et al.*[26,27] constructed a unique micro-CT system for three-dimensional *in vitro* analyses

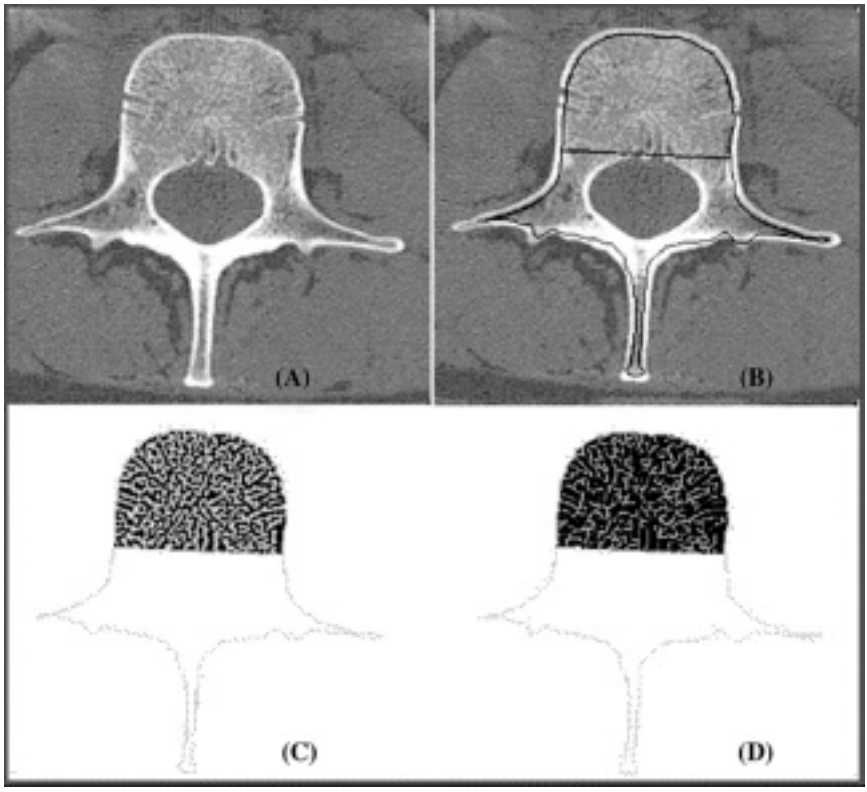

FIGURE 3. High-resolution spinal CT with post-processing steps used to access trabecular structure from CT image (**A**). The structure is segmented by defining the boundary between cortical and trabecular bone (**B**). The trabecular network is reduced to a binary image (**C**), which is then thinned to produce a representation of the trabecular from (**D**). (Courtesy of Christopher Gordon.)

of small bone samples. The system employed cone-beam geometry and a three-dimensional reconstruction algorithm. The spatial resolution of $\approx$60 μm clearly visualized individual trabeculae, allowing a three-dimensional analysis of trabecular network. Goulet *et al.*[28] used images of bone cubes generated by this system to examine standard histomorphometric parameters as well as additional parameters, such as Euler number, an index of connectivity, and mean intercept length, a means of determining anisotrophy. Goulet also related these image-based parameters to Young's modulus, a measure of elasticity of bone. Based on data sets from Feldkamp's micro-CT, Engelke *et al.*[29,30] developed a three-dimensional digital model of trabecular bone for comparing two- and three-dimensional structural analysis methods, and to investigate the effects of spatial resolution and image processing techniques on the extraction of structural parameters (FIG. 4). Three-dimensional data sets from these micro-CT

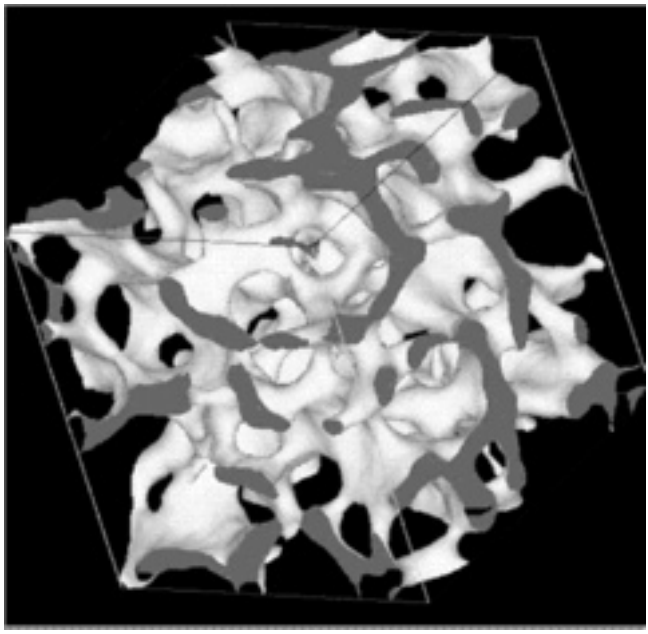

FIGURE 4. Three-dimensional digital model of trabecular bone based on micro-CT image at approximately 60 μm^3 resolution. (Courtesy of Klaus Engelke.)

systems can be used for calculating classical histomorphometric parameters like trabecular thickness and separation[31–33] as well as for determining topological measurements like the Euler number and connectivity.

Another *in vitro* micro-CT scanner with a spatial resolution of 15–20 μm^3 was developed by Rüeggsegger *et al*.[34,35] and has been used extensively in laboratory investigations. Its high accuracy in relation to standard two-dimensional histomorphometry as well as to serial grindings and their derived three-dimensional parameters has been reported.[16] The relationship of these parameters to *in vitro* measures of strength and their application to micro-finite-element modeling has been shown.[36,37] More recently, additional special purpose ultra-high-resolution micro-CT systems have been developed for imaging bone microstructure at resolutions approaching 10 μm or better.[38] These various micro-CT systems have found wide application in both preclinical animal studies and clinical research settings.[39] Similarly, in animal studies, micro-CT has recently found applications in the assessment of skeletal phenotype in gene knockout or in mice,[40–43] in osteoporotic[44] or arthritic rodents.[45]

In a human study by Jiang *et al*., the rapid deterioration in trabecular microarchitecture in women experiencing menopause was documented by paired iliac crest biopsies before and approximately 5 years after the menopause (FIG. 5). Prominent thinning of trabeculae and conversion of plate-like to rod-like trabecular structure were observed.[39]

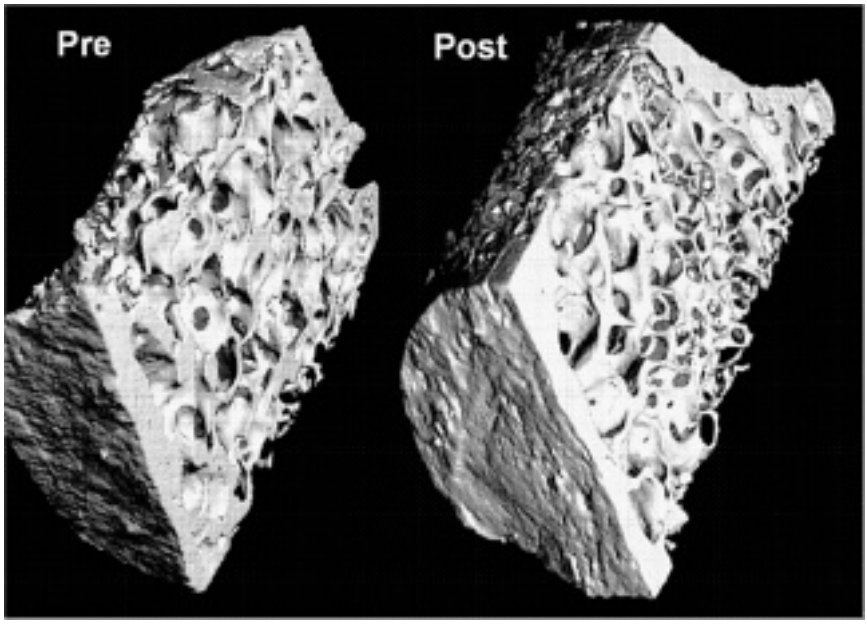

FIGURE 5. Micro-CT image at ~20 μm^3 resolution of trabecular structure of serial iliac crest biopsies from a postmenopausal woman before and 2 years after estrogen replacement therapy. (Courtesy of Yebin Jiang.)

Jiang *et al*. also used micro-CT with three-dimensional analyses compared to standard two-dimensional histomorphometry to study the longitudinal impact of teriparatide (PTH 1–34) treatment versus placebo on the skeleton of postmenopausal women (FIG. 6). In this analysis the changes of the more simple two-dimensional indices pertaining to cancellous bone structure, such as trabecular number, thickness, and spacing did not reach significance after PTH treatment. However, more stereologically correct indices, like marrow star volume and micro-CT-based three-dimensional indices, revealed significant changes, further corroborating the superiority of these techniques for structural analysis of small samples, like bone biopsies. The root mean square CV as reproducibility of micro-CT examination after rescanned and reanalyzed 20 human biopsy specimens was 2–6% for trabecular structural parameters.[46,47]

While the micro-CT scanners described above use an X ray tube as radiation source, other investigators have explored the potential of high-intensity, tight collimation synchrotron radiation, which allows either faster scanning or higher spatial resolution in imaging bone specimens. These systems have been referred to as X ray tomographic microscopy (XTM) and can achieve spatial resolution of 10 μm or better. Bonse, Graeff, and Engelke[18,48–50] were among the first to apply this approach to imaging of bone specimens. Kinney and Lane *et al.*[51,52] have applied the XTM approach to imaging the rat tibia at ultra

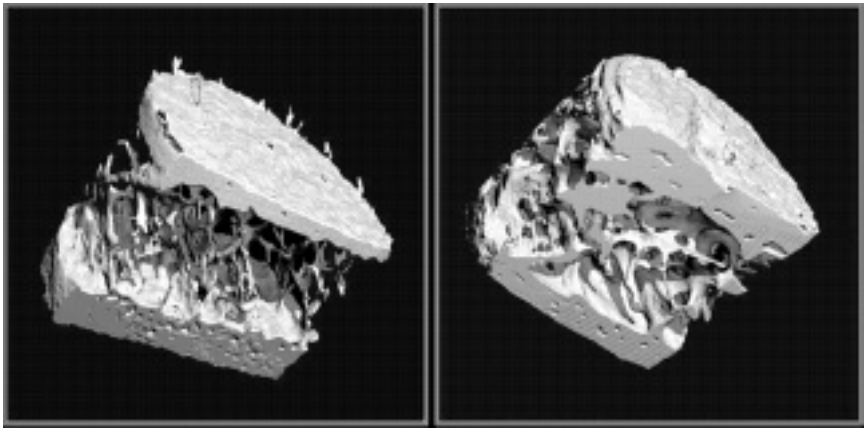

FIGURE 6. Paired biopsy sample was obtained from a 65-year-old woman treated with PTH. Compared to the baseline biopsy (**A**), PTH treatment (**B**) increased trabecular bone volume, trabecular connectivity, and cortical thickness, and shift trabecular morphology from a rod-like structure to a more plate-like pattern. (Courtesy of Yebin Jiang.)

high resolution, both *in vitro* and *in vivo*, and have documented the impact of oophorectomy and PTH treatment on two- and three-dimensionally derived trabecular bone indices. Ritman and Peyrin *et al.*[53] have used synchrotron-based XTM to image trabecular bone ultrastructure at resolutions approaching 1–2 μm, thereby providing the capability to assess additional features, such as resorption cavities. In recently reported studies using synchrotron radiation, micro-CT examination of sequential iliac biopsies showed that treatment with a bisphosphonate did not cause significant hypermineralization but did increase the mineralization at the tissue level.[54] Also, standard micro-CT and histomorphometric assessments of serial iliac crest bone biopsies from postmenopausal women treated with another bisphosphonate for 10 years showed normal microarchitecture.[55]

At recent international congresses there have been many additional studies using micro-CT, including technical developments and various applications. An *in vivo* human micro-CT scanner developed in Europe has been used to examine distal radius or distal tibia with isotropic resolution of about 100 μm.[56] Its application in United States and other places remains to be seen. Advanced micro-finite analyses with models based on these three-dimensional peripheral micro-CT systems (isotropic voxel resolution of 165 μm) have predicted the failure load of the human radius Colles fractures better than by DXA or bone morphology and geometry measurements.[57] Micro-CT (and micro-MRI, see below) replicate the complex trabecular architecture on a macroscopic scale for visual or biomechanical analysis. A complete set of three-dimensional image data provides a basis for finite-element modeling for virtual biomechanics to predict mechanical properties.[58]

MR MICROSCOPY

High-resolution MR and micro-MR—referred to collectively as MR microscopy—have received considerable attention as research tools and as potential clinical tools for assessment of trabecular bone architecture. Magnetic resonance is a complex technology based on the application of high-magnetic fields, transmission of radiofrequency (RF) waves, and detection of RF signals from excited hydrogen protons. A noninvasive, nonionizing radiation technique, MR can provide three-dimensional images in arbitrary orientations and can depict trabecular bone as a negative image by virtue of the strong signal generated by the abundant fat and water protons in the surrounding marrow tissue. The appearance of the MR image is affected by many factors beyond spatial resolution, including the field strength and specific pulse sequence used, the echo time, and the signal-to-noise achieved.[59–61] Analysis and interpretation of MR images are more complicated than for the X ray-based images of CT. Nevertheless, MR microscopy holds much promise for improved quantitative assessment of trabecular structure both *in vivo* and *in vitro*.

Because of the relation of signal-to-field strength in MR, special purpose, small bore, high-field magnets have been employed to obtain very high resolution or micro-MR images of bone specimens *in vitro*. Wehrli and colleagues[62–65] obtained 78-μm isotopic resolution of human and bovine bone cubes using three-dimensional imaging at 9.4 Tesla, and derived anisotropy ellipsoids from the analysis of mean intercept length. They also found good correlations between MR-derived parameters and standard histomorphometric measures. Antich *et al.*[66] have conducted similar experiments and found changes in accordance with histomorphometry measures. Kapadia *et al.*[67] extended the *in vitro* techniques to obtain images in an ovariectomized rat model and were able to measure changes in trabecular structure following ovariectomy. Hipp and colleague[68] examined bovine cubes in a small bore microimaging spectrometer at 60-μm^3 resolution and found three-dimensional results heavily dependent upon the threshold and image processing algorithm. Majumdar *et al*.[69] examined human cadaver specimens using a standard clinical MR scanner at 1.5 Tesla and a spatial resolution of $117 \times 117 \times 300$ μm, and compared these images with XTM images and with serial grindings to determine the impact of in-plane resolution and slice thickness on both two- and three-dimensional structural and textural parameters. Considerable resolution dependence was observed for traditional stereological parameters, some of which could be modulated by appropriate thresholds and image processing techniques.

Limitations of signal-to noise, spatial resolution, and total imaging time, prevent resolution of smaller individual trabeculae *in vivo* at clinical field strengths, but the images show the larger trabeculae and the texture of the trabecular network. The trabecular structure can still be quantified using standard techniques of stereology as well as textural parameters, such as fractal analysis.

In an early study by Majumdar *et al.*[60] establishing the feasibility of using such images to quantify trabecular structure, MR images of the distal radius were obtained using a modified gradient echo sequence, a 1.5 Tesla imager, and a spatial resolution of 156 μm^2 and slice thickness of 0.7 mm. Representative axial sections from normal and osteoporotic subjects clearly depicted the loss of the integrity of the trabecular network with the development of osteoporosis (FIG. 7). Similar images of the calcaneus of normal subjects showed that the orientation of the trabeculae is significantly different in various anatomic regions. Ellipses, representing the mean intercept length, showed a preferred orientation and hence mapped the anisotropy of trabecular structure. In preliminary *in vivo* studies of the calcaneus, *gray* scale reference values from fat, muscle, and tendon were used to calculate reproducible threshold values.[70] This approach gave a midterm, *in vivo* precision of ≈3.5% CV for trabecular width and spacing.

Both Wehrli and colleagues,[71] and Glüer and colleagues,[72–74] have used clinical imagers at 1.5 Tesla with special RF coil designs and have measured trabecular and cortical bone in the phalanges, a convenient anatomic site particularly suitable for obtaining high signal-to-noise and high-spatial resolution images *in vivo*. Resolution of 78–150 μm and slice thickness of 300 μm have been achieved in the phalanges. Stampa *et al.*[74] used these phalangeal images to derive quantitative three-dimensional parameters based on an algorithm and model for defining trabecular rods and plates. Others, including Link *et al.*,[75] Majumdar *et al.*[76] and Wehrli *et al.*[77–79] have shown the ability to discriminate spine and/or hip fractures using trabecular structure or textural parameters from *in vivo* MR images of the radius or calcaneus. Recently, Engelke has provided a comprehensive analysis of threshold effects in hrMR of the calcaneus when compared with ultra-high-resolution anatomic sectioning *in vitro*.[80] Newitt has reported promising results on the application of micro-finite-element analyses based on hrMR images of the distal radius *in vivo*.[81] Structure parameters determined in high-resolution MR images of the proximal femur specimen correlated significantly with bone strength, with the highest correlations obtained combining DXA BMD and structure measures.[82]

The resolution achievable *in vivo* by MRI is not sufficient to depict precisely individual trabeculae and, thus, does not permit the quantification of the "true" trabecular bone morphology and topology. Trabecular samples of the distal radius imaged using MRI at 156 × 156 × 300 μ correlate well with micro-CT at 34 × 34 × 34 μ, with r^2 ranging from 0.57 to 0.64 for morphological measurements.[83] Trabecular bone structure parameters assessed in the distal radius on high-resolution MR and multislice CT images are significantly correlated with those determined on contact radiographs of the corresponding specimen sections. For the MR imaging, the threshold algorithm used for binarizing the images substantially affected these correlations.[84]

In an animal study by Jiang *et al.*, MRI microscopy showed that ovariectomy induces deterioration of trabecular microstructure and of the biomechanical

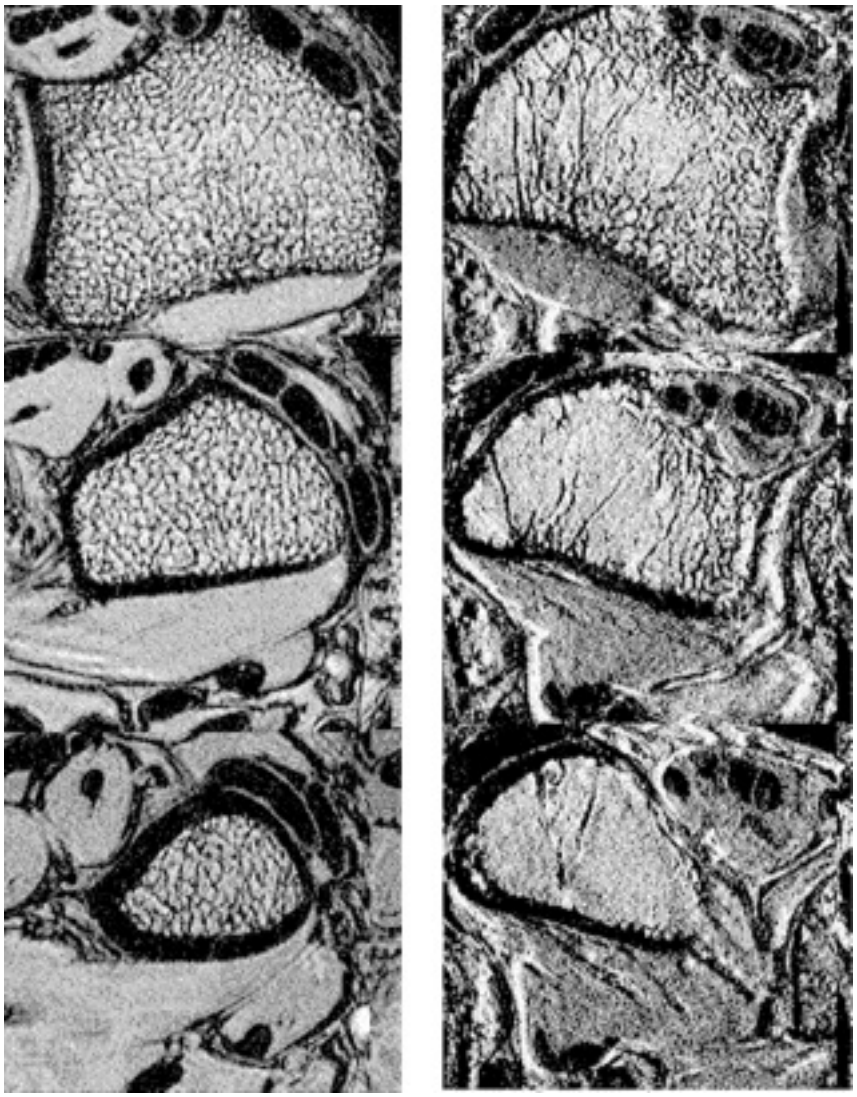

FIGURE 7. High-resolution (~150 × 150 × 500 μm) axial gradient echo MR images of the distal radius of a young woman (**L**) and an elderly osteoporotic woman (**R**) clearly show the deterioration in trabecular and cortical structure. (Courtesy of Sharmila Majumdar.)

properties in the femoral neck of ewes (FIG. 8). Calcitonin treatment prevented ovariectomy (OVX) induced changes in a dose-dependent manner. The femoral neck trabecular microstructure significantly correlates with biomechanical properties, and its combination with BMD further improved the prediction of bone quality.[85]

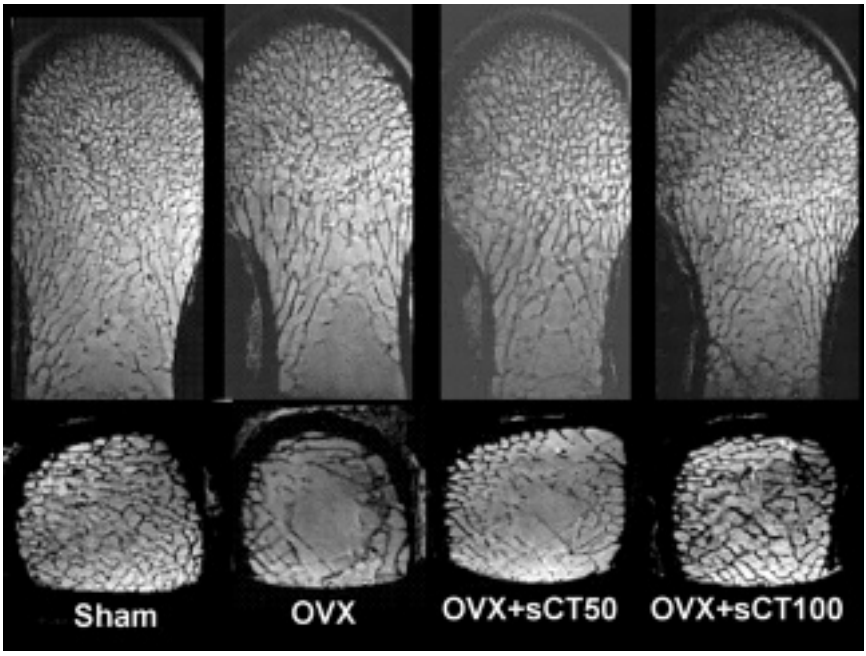

FIGURE 8. MR microscopic images of the proximal femur show that the ovariectomy (OVX)-induced loss in trabecular microstructure in the femoral neck is prevented by the treatment of salmon calcitonin (sCT) at 50 IU or 100 IU.

MR microscopic images of the proximal femur show that the OVX-induced loss in trabecular microstructure in the femoral neck is prevented by the treatment of salmon calcitonin (sCT) at 50 IU or 100 IU.

CHALLENGES FOR BONE IMAGING

Despite the considerable progress that has been made over the past decade in advanced bone imaging for osteoporosis assessment, a number of challenges remains. Technically, the challenges reflect the balances and trade-offs between spatial resolution, sample size, signal-to noise, radiation exposure and acquisition time, or between the complexity and expense of the imaging technologies versus their availability and accessibility. Clinically, the challenges for bone imaging include balancing the advantages of standard BMD information versus the more complex architectural features of bone, or the deeper research requirements of the laboratory versus the broader needs of clinical practice. The biological differences between the peripheral appendicular skeleton and the central axial skeleton and their impact on the relevant bone imaging methods must be further clarified. Finally, the relative merits of

these sophisticated imaging techniques must be weighed with respect to their applications as diagnostic procedures, requiring high accuracy or reliability, versus their applications as monitoring procedures, requiring high precision or reproducibility.

ACKNOWLEDGMENTS

This research work was adapted in part from Genant HK, Gordon C, Jiang Y, Lang TF, Link TM, Majumdar S. 1999. Advanced imaging of bone macro- and microstructure. Bone **25:** 149–152.

REFERENCES

1. Genant, H.K., K. Engelke, T. Fuerst, *et al*. 1996. Noninvasive assessment of bone mineral and structure: state of the art. J. Bone Miner. Res. **11:** 707–730.
2. Faulkner, K.G., C.E. Cann & B.H. Hasegawa. 1990. CT-derived finite element model to determine vertebral cortex strength. *In* Medical Imaging IC: Image Processing, Vol. 1233. M.H. Loew, Ed.: 194–202. SPIE Newport Beach, California.
3. Lang, T.F., G. Guglielmi, C. van Kuijk, *et al*. 2002. Measurement of bone mineral density at the spine and proximal femur by volumetric quantitative computed tomography and dual-energy X-ray absorptiometry in elderly women with and without vertebral fractures. Bone **30:** 247–250.
4. Keyak, J.H., S.A. Rossi, K.A. Jones & H.B. Skinner. 1998. Prediction of femoral fracture load using automated finite element modeling. J. Biomech. **31:** 125–133.
5. Lang, T.F., J. Li, S.T. Harris & H.K. Genant. 1999. Assessment of vertebral bone mineral density using volumetric quantitative computed tomography. J. Comp. Assist. Tomogr. **23:** 130–137.
6. Lang, T.F., J.H. Keyak, M.W. Heitz, *et al*. 1997. Volumetric quantitative computed tomography of the proximal femur: precision and relation to bone strength. Bone **21:** 101–108.
7. Lotz, J.C., T.N. Gerhart & W.C. Hayes. 1990. Mechanical properties of trabecular bone from the proximal femur: a quantitative CT study. J. Comp. Assist. Tomogr. **14:** 107–114.
8. McBroom, R.J., W.C. Hayes, W.T. Edwards, *et al*. 1985. Prediction of vertebral body compressive fracture using quantitative computed tomography. J. Bone Joint Surg. Am. **67:** 1206–1214.
9. Jergas, M., M. Breitenseher, C.C. Glüer, *et al*. 1995. Estimates of volumetric bone density from projectional measurements improve the discriminatory capability of dual X-ray absorptiometry. J. Bone Miner. Res. **10:** 1101–1110.
10. Sode, M., J. Keyak, M. Bouxsein & T. Lang. 2004. Assessment of femoral neck torsional strength indices. J. Bone Miner. Res. **19:** S238.
11. Lang, T.F., J.H. Keyak, A. Yu, *et al*. 2003. Determinants of proximal femoral strength in elderly women. J. Bone Miner. Res. **18:** S266.
12. Crawford, R.P., C.E. Cann & T.M. Keaveny. 2003. Finite element models predict in vitro vertebral body compressive strength better than quantitative computed tomography. Bone **33:** 744–750.

13. CRAWFORD, R.P., W.S. ROSENBERG & T.M. KEAVENY. 2003. Quantitative computed tomography-based finite element models of the human lumbar vertebral body: effect of element size on stiffness, damage, and fracture strength predictions. J. Biomech. Eng. **125:** 434–438.
14. CHEVALIER, F., A.M. LAVAL-JEANTET, M. LAVAL-JEANTET, *et al*. 1992. CT image analysis of the vertebral trabecular network in vivo. Calcif. Tissue Int. **51:** 8–13.
15. ITO, M., M. OHKI, K. HAYASHI, *et al*. 1995. Trabecular texture analysis of CT images in the relationship with spinal fracture. Radiology **194:** 55–59.
16. GORDON, C.L., T.F. LANG, P. AUGAT, *et al*. 1998. Image-based assessment of spinal trabecular bone structure from high-resolution CT images. Osteoporos. Int. **8:** 317–325.
17. JIANG, Y., J. ZHAO, P. AUGAT, *et al*. 1998. Trabecular bone mineral and calculated structure of human bone specimens scanned by peripheral quantitative computed tomography: relation to biomechanical properties. J. Bone Miner. Res. **13:** 1783–1790.
18. LINK, T.M., V. VIETH, C. STEHLING, *et al*. 2003. High-resolution MRI vs multislice spiral CT: which technique depicts the trabecular bone structure best? Eur. Radiol. **13:** 663–671.
19. DURAND, E.P. & P. RÜEGSEGGER. 1992. High-contrast resolution of CT images for bone structure analysis. Med. Phys. **19:** 569–573.
20. MÜLLER, R., M. HAHN, M. VOGEL, *et al*. 1996. Morphometric analysis of noninvasively assessed bone biopsies: comparison of high-resolution computed tomography and histologic sections. Bone **18:** 215–220.
21. MÜLLER, R., T. HILDEBRAND, H.J. HAUSELMANN & P. RUEGSEGGER. 1996. In vivo reproducibility of three-dimensional structural properties of noninvasive bone biopsies using 3D-pQCT. J. Bone Miner. Res. **11:** 1745–1750.
22. ENGELKE, K., W. GRAEFF, L. MEISS, *et al*. 1993. High spatial resolution imaging of bone mineral using computed microtomography. Comparison with microradiography and undecalcified histologic sections. Invest. Radiol. **28:** 341–349.
23. TAKADA, M., K. KIKUCHI, S. UNAU & K. MURATA. 2004. Three-dimensional analysis of trabecular bone structure of human vertebra in vivo using image data from multi-detector row computed tomography—correlation with bone mineral density and ability to discriminate women with vertebral fracture. J Bone Miner. Res. **19:** S371.
24. BAUER, J.S., D. MUELER, M. FISCHBECK, *et al*. 2004. High resolution spiral-CT for the assessment of osteoporosis: which site of the spine and region of the vertebra is best suited to obtain trabecular bone structural parameters? J. Bone Miner. Res. **19:** S169.
25. KHOSLA, S., L.J. MELTON, E.J. ATKINSON, *et al*. 2004. Relationship of volumetric density, geometry and bone structure at different skeletal sites to sex steroid levels in men. J. Bone Miner. Res. **19:** S88.
26. FELDKAMP, L.A., S.A. GOLDSTEIN, A.M. PARFITT, *et al*. 1989. The direct examination of three-dimensional bone architecture in vitro by computed tomography. J. Bone Miner. Res. **4:** 3–11.
27. KUHN, J.L., S.A. GOLDSTEIN, L.A. FELDKAMP, *et al*. 1990. Evaluation of a microcomputed tomography system to study trabecular bone structure. J. Orthop. Res. **8:** 833–842.
28. GOULET, R.W., S.A. GOLDSTEIN, M.J. CIARELLI, *et al*. 1994. The relationship between the structural and orthogonal compressive properties of trabecular bone. J. Biomech. **27:** 375–389.

29. ENGELKE, K., C. KLIFA, B. MUNCH, *et al*. 1994. Morphological analysis of the trabecular network: the influence of image processing technique on structural parameters. 10th International Bone Densitometry Workshop, Venice Italy. J. Bone Miner. Res. **25:** S8.
30. ENGELKE, K., S.M. SONG, C.C. GLÜER & H.K. GENANT. 1996. A digital model of trabecular bone. J. Bone Miner. Res. **11:** 480–489.
31. PARFITT, A.M., C. MATTHEWS, A. VILLANUEVA. 1983. Relationships between surface, volume and thickness of iliac trabecular bone in aging and in osteoporosis. J. Clin. Invest. **72:** 1396–1409.
32. PARFITT, A.M. 1983. The stereologic basis of bone histomorphometry. Theory of quantitative microscopy and reconstruction of the third dimension. *In* Bone Histomorphometry: Techniques and Interpretations. R. Recker, Ed.: 53–87. CRC Press. Boca Raton.
33. ODGAARD, A. & H.J.G. GUNDERSEN. 1993. Quantification of connectivity in cancellous bone, with special emphasis on 3-D reconstructions. Bone **14:** 173–182.
34. RÜEGSEGGER, P., B. KOLLER & R. MULLER. 1996. A microtomographic system for the nondestructive evaluation of bone architecture. Calcif. Tissue Int. **58:** 24–29.
35. MÜLLER, R., F. BAUSS, S.Y. SMITH & M.K. HANNAN. 2001. Mechano-structure relationships in normal, ovariectomized and Ibandronate treated aged macaques as assessed by micro-tomographic imaging and biomechanical testing. Trans. Orthop. Res. Soc. **26:** 66.
36. MÜLLER, R. & P. RUEGSEGGER. 1996. Analysis of mechanical properties of cancellous bone under conditions of simulated bone atrophy. J. Biomech. **29:** 1053–1060.
37. VAN RIETBERGEN, B., H. WEINANS, R. HUISKES & A. ODGAARD. 1995. A new method to determine trabecular bone elastic properties and loading using micromechanical finite-element models. J. Biomech. **28:** 69–81.
38. ENGELKE, K., M. KAROLCZAK, S. SCHALLER, *et al*. 1998. A cone beam microcomputed tomography (μCT) system for imaging of 3D trabecular bone structure. Presented at the 13th International Bone Densitometry Workshop, 4–8 October, Wisconsin, USA.
39. JIANG, Y., P. ZHAO, E.Y. LIAO, *et al*. 2005. Application of micro CT assessment of 3D bone microstructure in preclinical and clinical studies. J. Bone Miner. Metab. (In press).
40. SOHASKEY, M.L., Y. JIANG, J. ZHAO, *et al*. 2004. Insertional mutagenesis of osteopotentia, a novel transmembrane protein essential for skeletal integrity. J. Bone Miner. Res. **19:** S21.
41. SOROCÉANU, M.A., D. MIAO, Y. JIANG, *et al*. 2004. *Pthrp* haploinsufficiency impairs bone formation but potentiates the bone anabolic effects of PTH (1-34). J. Bone Miner. Res. **19:** S97.
42. TAKESHITA, S., N. NAMBA, J. ZHAO, *et al*. 2002. SHIP-deficient mice are severely osteoporotic due to increased numbers of hyper-resorptive osteoclasts. Nat. Med. **8:** 943–949 (Online published on Aug. 5, 2002).
43. BERGO, M.O., B. GAVINO, J. ROSS, *et al*. 2002. Zmpste24 deficiency in mice causes spontaneous bone fractures, muscle weakness, and a prelamin A processing defect. Proc. Natl. Acad. Sci. USA **99:** 13049–13054.
44. LANE, N.E., M. BALOOCH, J. ZHAO, *et al*. 2004. Glucocorticoids induce changes around the osteocyte lacunae that reduces bone strength and bone mineral content independent of apoptosis: preliminary data from a glucocorticoid-induced bone loss model in male mice. J. Bone Miner. Res. **19:** S434–S435.

45. JIANG, Y., J.J. ZHAO, R. MANGADU, *et al*. 2004a. Assessment of 3D cortical and trabecular bone microstructure and erosion on micro CT images of a murine model of arthritis. J. Bone Miner. Res. **19:** S474.
46. JIANG, Y., J. ZHAO, B.H. MITLAK, *et al*. 2003. Recombinant human parathyroid hormone (1–34) (teriparatide) improves both cortical and cancellous bone structure. J. Bone Miner. Res. **18:** 1932–1941.
47. JIANG, Y., J. ZHAO, E.F. ERIKSEN & H.K. GENANT. 2003b. Reproducibility of micro CT quantification of 3D microarchitecture of the trabecular and cortical bone in the iliac crest of postmenopausal osteoporotic women and their treatment with teriparatide [rhPTH(1-34)]. RSNA **03:** 571.
48. BONSE, U., F. BUSCH, O. GUNNEWIG, *et al*. 1994. 3D computed x-ray tomography of human cancellous bone at 8 μm spatial and 10–4 energy resolution. Bone Miner. **25:** 25–38.
49. ENGELKE, K., W. DIX, W. GRAEFF, *et al*. 1991. Quantitative microtomography and microradiography of bones using synchrotron radiation. Presented at the 8th International Workshop on Bone Densitometry. Bad Reichenhall, Germany, Osteoporos. Int.
50. GRAEFF, W. & K. ENGELKE. 1991. Microradiography and microtomography. *In* Handbook on Synchrotron Radiation. S. Ebashi, M. Koch, E. Rubenstein, Eds.: 361–405. North-Holland, Amsterdam.
51. KINNEY, J.H., N.E. LANE & D.L. HAUPT. 1995. In vivo, three-dimensional microscopy of trabecular bone. J. Bone Miner. Res. **10:** 264–270.
52. LANE, N.E., J.M. THOMPSON, G.J. STREWLER & J.H. KINNEY. 1995. Intermittent treatment with human parathyroid hormone (hPTH[1–34]) increased trabecular bone volume but not connectivity in osteopenic rats. J. Bone Miner. Res. **10:** 1470–1477.
53. PEYRIN, F., M. SALOME, P. CLOETENS, *et al*. 1998. What do micro-CT examinations reveal at various resolutions: a study of the same trabecular bone samples at the 14, 7, and 2 micron level. Presented at the Symposium on Bone Architecture and the Competence of Bone. Ittingen, Switzerland, 3–5 July.
54. BORAH, B., E.L. RITMAN, T.E. DUFRESNE, *et al*. 2004. Five year risedronate therapynormalizes mineralization: synchrotron radiation micro-computed tomography study of sequential triple biopsies. J. Bone Miner. Res. **19:** S308.
55. RECKER, R., K. ENSRUD, S. DIEM, *et al*. 2004. Normal bone histomorphometry and 3D microarchitecture after 10 years alendronate treatment of postmenopausal women. J. Bone Miner. Res. **19:** S45.
56. NEFF, M., M. DAMBACHER, S. HAEMMERLE, *et al*. 2004. 3D evaluation of bone microarchitecture in humans using high resolution pQCT; a new in vivo, non invasive and time saving procedure. J. Bone Miner. Res. **19:** S236.
57. PISTOIA, W., B. VAN RIETBERGEN, E.M. LOCHMULLER, *et al*. 2002. Estimation of distal radius failure load with micro-finite element analysis models based on three-dimensional peripheral quantitative computed tomography images. Bone **30:** 842–848.
58. BORAH, B., G.J. GROSS, T.E. DUFRESNE, *et al*. 2001. Three-dimensional microimaging (MRmicroI and microCT), finite element modeling, and rapid prototyping provide unique insights into bone architecture in osteoporosis. Anat. Rec. **15:** 101–110.
59. MAJUMDAR, S., H. GENANT, A. GIES & G. GUGLIELMI. 1993. Regional variations in trabecular structure in the calcaneus assessed using high resolution magnetic resonance images and quantitative image analysis. J. Bone Miner. Res. **8S:** 351.

60. MAJUMDAR, S., H. GENANT, S. GRAMPP, *et al*. 1994. Analysis of trabecular bone structure in the distal radius using high resolution MRI. Eur. Radiol. **4:** 517–524.
61. MAJUMDAR, S., D.C. NEWITT, M. JERGAS, *et al*. 1995. Evaluation of technical factors affecting the quantification of trabecular bone structure using magnetic resonance imaging. Bone **17:** 417–430.
62. CHUNG, H., F.W. WEHRLI, J.L. WILLIAMS & S.D. KUGELMASS. 1993. Relationship between NMR transverse relaxation, trabecular bone architecture, and strength. Proc. Natl. Acad. Sci. USA **90:** 10250–10254.
63. CHUNG, H.W., F.W. WEHRLI, J.L. WILLIAMS, *et al*. 1995. Quantitative analysis of trabecular microstructure by 400 MHz nuclear magnetic resonance imaging. J. Bone Miner. Res. **10:** 803–811.
64. CHUNG, H.W., F.W. WEHRLI, J.L. WILLIAMS & S.L. WEHRLI. 1995. Three-dimensional nuclear magnetic resonance microimaging of trabecular bone. J. Bone Miner. Res. **10:** 1452–1461.
65. HWANG, S.N., F.W. WEHRLI & J.L. WILLIAMS. 1997. Probability-based structural parameters from three-dimensional nuclear magnetic resonance images as predictors of trabecular bone strength. Med. Phys. **24:** 1255–1261.
66. ANTICH, P., R. MASON, R. MCCOLL, *et al*. 1994. Trabecular architecture studies by 3D MRI microscopy in bone biopsies. J. Bone Miner. Res. **9S1:** 327.
67. KAPADIA, R.D., W. HIGH, D. BERTOLINI & S.K. SARKAR. 1993. MR microscopy: a novel diagnostic tool in osteoporosis research. *In* 4th International Symposium on Osteoporosis & Consensus Development Conference. C. Christiansen, Ed.: 28. Hong Kong.
68. SIMMONS, C.A. & J.A. HIPP. 1997. Method-based differences in the automated analysis of the three-dimensional morphology of trabecular bone. J. Bone Miner. Res. **12:** 942–947.
69. MAJUMDAR, S., D. NEWITT, A. MATHUR, *et al*. 1996. Magnetic resonance imaging of trabecular bone structure in the distal radius: relationship with X-ray tomographic microscopy and biomechanics. Osteoporos. Int. **6:** 376–385.
70. OUYANG, X., K. SELBY, P. LANG, *et al*. 1997. High resolution magnetic resonance imaging of the calcaneus: age-related changes in trabecular structure and comparison with dual X-ray absorptiometry measurements. Calcif. Tissue Int. **60:** 139–147.
71. JARA, H., F.W. WEHRLI, H. CHUNG & J.C. FORD. 1993. High-resolution variable flip angle 3D MR imaging of trabecular microstructure in vivo. Magn. Reson. Med. **29:** 528–539.
72. KÜHN, B., B. STAMPA & C.C. GLÜER. 1997. Hochauflösende Darstellung und Quantifierung der trabekulären Knochenstruktur der Fingerphalangen mit der Magnetresonanztomographie. Z. Med. Phys. **7:** 162–168.
73. STAMPA, B., B. KÜHN, M. HELLER, C.C. GLÜER. 1998. Rods or plates: a new algorithm to characterize bone structure using 3D magnetic resonance imaging. Presented at the 13th International Bone Densitometry Workshop, 4–8 October. Wisconsin, USA.
74. STAMPA, B., B. KUHN, C. LIESS, *et al*. 2002. Characterization of the integrity of three-dimensional trabecular bone microstructure by connectivity and shape analysis using high-resolution magnetic resonance imaging in vivo. Top. Magn. Reson. Imaging **13:** 357–363.
75. LINK, T., S. MAJUMDAR, P. AUGAT, *et al*. 1998. In vivo high resolution MRI of the calcaneus: differences in trabecular structure in osteoporotic patients. J. Bone Miner. Res. **13:** 1175–1182.

76. MAJUMDAR, S., H.K. GENANT, S. GRAMPP, *et al*. 1997. Correlation of trabecular bone structure with age, bone mineral density and osteoporotic status: in vivo studies in the distal radius using high resolution magnetic resonance imaging. J. Bone Miner. Res. **12:** 111–118.
77. WEHRLI, F.W., S.N. HWANG, J. MA, *et al*. 1998. Cancellous bone volume and structure in the forearm: noninvasive assessment with MR microimaging and image processing. Radiology **206:** 347–357.
78. WEHRLI, F.W., B.R. GOMBERG, P.K. SAHA, *et al*. 2001. Digital topological analysis of in vivo magnetic resonance microimages of trabecular bone reveals structural implications of osteoporosis. J. Bone Miner. Res. **16:** 1520–1531.
79. WEHRLI, F.W., P.K. SAHA, B.R. GOMBERG, *et al*. 2002. Role of magnetic resonance for assessing structure and function of trabecular bone. Top. Magn. Reson. Imaging **13:** 335–355.
80. ENGELKE, K., M. HAHN, M. TAKADA, *et al*. 2001. Structural analysis of high resolution in vitro MR images compared to stained grindings. Calcif. Tissue Int. **68:** 163–171.
81. NEWITT, D.C., S. MAJUMDAR, B. VAN RIETBERGEN, *et al*. 2002. In vivo assessment of architecture and micro-finite element analysis derived indices of mechanical properties of trabecular bone in the radius. Osteoporos. Int. **13:** 6–17.
82. LINK, T.M., V. VIETH, R. LANGENBERG, *et al*. 2003. Structure analysis of high resolution magnetic resonance imaging of the proximal femur: in vitro correlation with biomechanical strength and BMD. Calcif. Tissue Int. **72:** 156–165.
83. POTHUAUD, L., A. LAIB, P. LEVITZ, *et al*. 2002. Three-dimensional-line skeleton graph analysis of high-resolution magnetic resonance images: a validation study from 34-microm-resolution microcomputed tomography. J. Bone Miner. Res. **17:** 1883–1895.
84. LINK, T.M., V. VIETH, C. STEHLING, *et al*. 2003. High-resolution MRI vs multislice spiral CT: which technique depicts the trabecular bone structure best? Eur. Radiol. **13:** 663–671.
85. JIANG, Y., J. ZHAO, P. GEUSENS, *et al*. 2005. Femoral neck trabecular microstructure in ovariectomized ewes treated with calcitonin: MRI microscopic evaluation. J. Bone Miner. Res. **20:** 125–130.